

Temperature Dependence of the Outer-Sphere Reorganization Energy

Daniel L. Derr and C. Michael Elliott*

Department of Chemistry, Colorado State University, Fort Collins, Colorado 80523

Received: May 27, 1999; In Final Form: August 2, 1999

The temperature dependence of the intervalence charge transfer transition (IT) has been studied for a mixed-valence dinuclear iron complex. The two “halves” of this complex consist of trisbipyridineiron moieties that are triply linked with saturated alkyl chains. Because the complex is symmetric, the energy of the IT band is a direct measure of the reorganization energy for electron transfer between the two irons. Moreover, for the specific complex under investigation here, the inner-sphere reorganization energy is essentially zero because of an exact cancellation of sigma- and pi-bonding changes upon changing the oxidation state of each iron. As a consequence, the energy of the IT transition is a direct measure of the outer-sphere (solvent) reorganization energy. The energy of the IT band has been investigated over the temperature range $-28\text{ }^{\circ}\text{C}$ to $30\text{ }^{\circ}\text{C}$. The derivative of the outer-sphere reorganization energy with respect to temperature found from this study was $-3.2 \pm 0.4\text{ cm}^{-1}\text{K}^{-1}$. Theoretical calculations based on the Marcus two spheres in a dielectric continuum model and a molecular based model developed by Matyushov were also carried out for comparison with the experimental results. The continuum model predicts a positive slope for the derivative while the Matyushov model gives a negative slope that differs from that of the experimental data by a factor of ~ 2 in magnitude.

Introduction

Over temperature ranges that are usually accessible for solution phase electron transfer (ET) reactions, the temperature dependence of the total reorganization energy (λ) is usually small and is often neglected.¹ The small temperature dependence that does exist predominantly arises from the solvent contribution to the reorganization energy.²

While in an absolute sense the temperature-dependent variations in λ are small, there are instances in which even small variations are of considerable consequence.^{3,4} Consider, for example, the situation of determining the donor–acceptor coupling matrix element (H_{12}) from temperature-dependent rates of electron self-exchange. For a nonadiabatic system at the high-temperature limit, Levich developed eq 1 to describe the relationship between k_{ET} (the electron-transfer rate constant), H_{12} , and λ .⁵

$$k_{\text{ET}} = \frac{2(H_{12})^2}{h} \sqrt{\frac{\pi^3}{\lambda kT}} \exp(-\lambda/4kT) \quad (1)$$

In this equation, λ occurs in both the preexponential term and the exponent. The way the temperature dependence of λ is treated will affect k_{ET} through both of these terms. The absolute variation in λ with T is small and the effects from the preexponent are negligible, but those in the exponent are not. Proceeding with this assumption and rearranging eq 1 gives⁴

$$\ln(k_{\text{ET}} \sqrt{T}) = A + B\left(\frac{1}{T}\right) \quad (2)$$

where

* Corresponding author.

$$A = \ln\left(\frac{2(H_{12})^2}{h} \sqrt{\frac{\pi^3}{\lambda k(T_0)}}\right) - \frac{1}{4k}\left(\frac{\partial\lambda}{\partial T}\right)_P \quad (3)$$

and

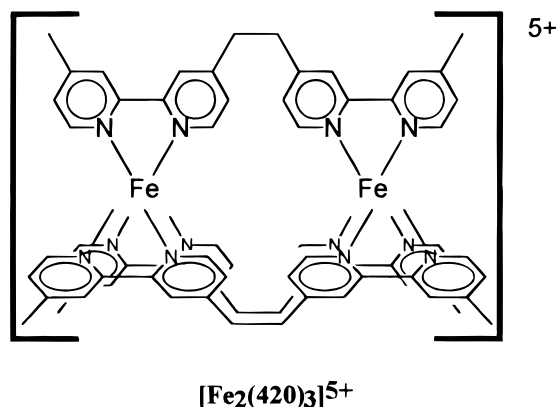
$$B = -\frac{\lambda(T_0)}{4k} - \frac{T_0}{4k}\left(\frac{\partial\lambda}{\partial T}\right)_P \quad (4)$$

assuming $(\partial\lambda/\partial T)_P$ is constant over the relevant temperature range. T_0 is the temperature in Kelvin within the experimental temperature range at which $(\partial\lambda/\partial T)_P$ is evaluated. Equations 2–4 indicate that H_{12} can, in principle, be determined from the intercept of an Arrhenius-type plot of $\ln(k_{\text{ET}}(T)^{1/2})$ vs $1/T$. In practice, the temperature range over which values of k_{ET} can be measured is usually narrow relative to the distance between the highest temperature data point and the ordinate of the plot. For example, the range of $1/T$ over which acetonitrile is a liquid is only ca. half as wide as the range between $1/T$ at the boiling point of acetonitrile and $1/T = 0$ (K^{-1}). Consequently, small variations in the slope of the plot produce large variations in the intercept, and ignoring even a small temperature dependence of λ can potentially produce significant error in H_{12} . Such circumstances therefore require that the temperature dependence of λ be confronted.^{3,4}

We describe here the results of an investigation of the intervalence charge transfer transition (IT) band for the mixed valence system $[\text{Fe}_2(420)_3]^{5+}$ in acetonitrile- d_3 . As will be demonstrated below, the energy of the IT band for this complex gives directly the outer-sphere reorganization energy from which its temperature dependence has been determined.

Experimental Section

Materials and Instrumentation. $[\text{Fe}_2(420)_3](\text{PF}_6)_4$ was prepared as previously reported.⁸ Except as noted, all other



chemicals were used as purchased from Aldrich Chemical Co., Fisher Scientific Co., Elf Atochem, or McCormick Distilling Co. Acetonitrile-*d*₃ (Cambridge Isotope Laboratories, Andover, MA) was the solvent used in the spectral titrations. Nitrosonium tetrafluoroborate (Aldrich) was vacuum-dried and stored under inert atmosphere before use. Near-IR spectra were obtained on a Varian Cary 2400 spectrophotometer that was purged with argon. The instrument was controlled by Spectra Calc (Galactic Industries, Salem, NH) software on an interfaced computer. In the variable temperature experiments, temperature was controlled with an Isotemp 1013s (Fisher Scientific, Pittsburgh, PA) circulating bath.

[Fe(TMP)₃](PF₆)₂. A solution of 250 mg ferrous ammonium sulfate hexahydrate (6.37×10^{-4} mol) in 50 mL water was added with stirring to a solution of 500 mg 3,4,7,8-tetramethyl-1,10-phenanthroline (TMP, 2.12 mmol) in 50 mL absolute ethanol. A dark red-orange color was immediately evident. The ethanol was removed by rotary evaporation whereupon the excess ligand precipitated. It was removed by filtration and washed three times with distilled water. The filtrate and washes were combined and treated with excess ammonium hexafluorophosphate, producing a dark red-orange precipitate. This precipitate was filtered, washed 3 times each with water, toluene and ether, and dried under vacuum. Yield was 670 mg (100%). ¹H NMR (ACN-*d*₃, 25 °C): δ 8.34 (s, 6H), 7.27 (s, 6H), 2.77 (s, 18H), 2.18 (s, 18H). Visible spectrum (ACN, λ , nm (ϵ , M⁻¹ cm⁻¹)): 501 (11 000), 475 shoulder (10 000).

Room-Temperature Titration. A 0.020 M solution of [Fe₂(420)₃](PF₆)₄ was prepared in an inert atmosphere box by dissolving 127 mg (7.09×10^{-5} mol) of the complex in acetonitrile-*d*₃ from three sealed 1 g vials. The dark red solution of [Fe₂(420)₃]⁴⁺ was treated with 16.5 mg (1.41×10^{-4} mol) of the oxidizing agent NOBF₄, resulting in a dark green solution of [Fe₂(420)₃]⁶⁺. Once the oxidation was complete (several hours), the solution was purged with N₂ to remove any dissolved, residual nitric oxide. This was accomplished by repeatedly filling a disposable pasture pipet with box atmosphere and discharging it through the solution. The entire solution was filtered through a pasture pipet containing a cotton plug and a small layer of Celite into a 1 cm path length quartz cell. The redox titration was carried out by adding a total of 128 mg of solid [Fe(TMP)₃](PF₆)₂ (1.41×10^{-4} mol) as the reducing agent which had been divided into six aliquots. During the entire procedure the cell remained within the Ar purged cell compartment of the spectrometer to minimize contact with atmospheric moisture. A total of seven spectra were taken over the range 2900 to 801 nm, one at each point in the titration. The temperature of the spectrometer cell compartment was maintained at 30 °C.

Variable Temperature Titration. Variable temperature experiments were conducted employing a 5 cm path length cell with a volume of ~ 5 mL. The cell was jacketed to allow flowing thermostated liquid to bathe the entire cell body except for the optical windows. The windows were constructed of double pairs of quartz plates separated by an evacuated space to minimize condensation at subambient temperatures. Otherwise, the variable temperature titration was similar to the isothermal one. The initial solution was prepared by oxidizing 179 mg [Fe₂(420)₃](PF₆)₄ (9.99×10^{-5} mol) with 23 mg nitrosonium tetrafluoroborate (1.96×10^{-4} mol). A total of 175 mg [Fe(TMP)₃](PF₆)₂ (1.94×10^{-4} mol) titrant was required which was added as the solid in four approximately equal portions. Again, each addition of [Fe(TMP)₃](PF₆)₂ was carried out at 30 °C with the cell remaining in the argon purged cell compartment. At each of the five points of the titration, spectra were obtained (2150 to 801 nm) at bath temperatures of 30, 15, 0, -15, and -30 °C, in that order. After the final temperature-dependent spectra of the titration were obtained, the actual temperatures in the cell at these bath temperatures was determined with a Fluke 51 K/J thermometer with a K-type thermocouple inserted directly into the cell.

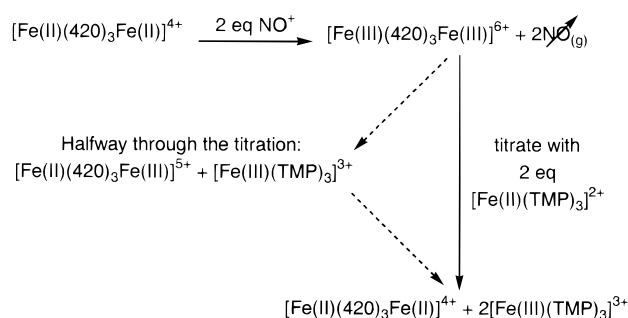
Results and Discussion

[Fe₂(420)₃]⁵⁺ is an excellent candidate for a study of temperature effects in the outer-sphere reorganization energy for several reasons. First, this complex is a symmetric, mixed valence species, thus the reorganization energy can be experimentally determined directly from the energy of the IT band.⁷ Also, the IT band is not obscured by any strong absorbances of the two individual chromophores ([Fe(bpy)₃]²⁺ and [Fe(bpy)₃]³⁺ where bpy is 2,2'-bipyridine). For a more in-depth discussion of these spectra, see the Supporting Information and ref 4). Second, the electron-transfer reaction associated with the IT event is thermoneutral and no consideration of the temperature dependence of ΔG is required. Since the value of $(\partial\lambda/\partial T)_P$ appears to be of the same magnitude (vide infra) as $(\partial(\Delta G)/\partial T)_P$ for many asymmetric systems that have been investigated,¹ this feature provides an important simplification in the data treatment.

Because of an apparent exact cancellation between changes in sigma and pi bonding of the metal and the bipyridine ligand when the oxidation state of the iron is changed from 2+ to 3+, the inner-sphere component of the total reorganization energy (λ_i) for [Fe₂(420)₃]⁵⁺ is effectively zero. Crystallographic and vibrational data substantiating this assertion are discussed thoroughly in refs 4 and 8. The inner-sphere reorganization is typically assumed to be temperature independent,^{1,9} and thus not to contribute to $(\partial\lambda/\partial T)_P$, the consequence of which is that the total reorganization energy is due solely to low frequency solvent motions that may be treated classically (i.e., as in eq 1).^{1,9} In other words, the energy of the IT band of [Fe₂(420)₃]⁵⁺ is a direct measure of the outer-sphere reorganization energy (λ_o).

Finally, the coupling of the donor and acceptor orbitals in [Fe₂(420)₃]⁵⁺ is notably weaker than in the vast majority¹⁰ of mixed-valence complexes that are typically studied ($H_{12} = 20$ cm⁻¹).⁸ The assumption of nonadiabaticity in the intramolecular electron transfer is, therefore, almost rigorously valid. Unfortunately, this means the complex's IT transition is quite weak ($\epsilon = 2$ M⁻¹cm⁻¹), and extracting the IT spectrum from the background requires careful spectral subtractions and judicious choices of solvent and redox reagents.⁸ When done properly, quantitatively reliable spectra for systems even more weakly coupled than [Fe₂(420)₃]⁵⁺ are obtained.⁴ However, evaluating

SCHEME 1



data from such weak transitions requires special caution because spectral phenomena which have negligible impacts on stronger IT transitions become relatively more important as $\epsilon \rightarrow 0$. Generally, to have confidence in the results when dealing with very weak IT transitions, we have found it useful to over-determine the system. For example, in the present case, rather than simply preparing a single solution at a single concentration of $[\text{Fe}_2(\text{420})_3]^{5+}$, a solution of $[\text{Fe}_2(\text{420})_3]^{6+}$ was titrated through the $[\text{Fe}_2(\text{420})_3]^{5+}$ form to $[\text{Fe}_2(\text{420})_3]^{4+}$ with data collected at several intermediate concentrations over the course of the titration. In this way multiple independent measurements of the IT band of $[\text{Fe}_2(\text{420})_3]^{5+}$ were obtained at each temperature and from solutions of different relative compositions of $[\text{Fe}_2(\text{420})_3]^{4+}$, $[\text{Fe}_2(\text{420})_3]^{5+}$, and $[\text{Fe}_2(\text{420})_3]^{6+}$.

Choice of Solvent, Oxidant, and Reductant. From the earlier spectral study of $[\text{Fe}_2(\text{420})_3]^{5+}$ reported in ref 8 approximate values of ν_{IT} and ϵ in acetonitrile were known. From a chemical standpoint acetonitrile is an excellent solvent for these studies because it has a high dielectric constant, the complex is rather soluble in all three relevant oxidation states over a wide range of temperatures, and all three oxidation states are stable for extended periods. However, spectrally acetonitrile is a rather poor solvent for these studies because of its relatively strong vibrational overtone transitions in the energy region of the IT band. Deuterating the solvent shifts these transitions to lower energies, minimizing their interference with the IT band; therefore, acetonitrile- d_3 was used in all the spectral titrations.

In our earlier spectral examination of $[\text{Fe}_2(\text{420})_3]^{5+}$ the as-synthesized $[\text{Fe}_2(\text{420})_3]^{4+}$ complex was titrated directly in the spectral cell by adding aliquots of solid NOBF_4 as an oxidant.⁸ This approach is simple but it has a drawback: the NO formed from the reduction of NO^+ is oxidized by atmospheric O_2 to various NO_x products which have significant absorbances in the spectral region of the IT band. To avoid this problem in the present experiments, the $[\text{Fe}_2(\text{420})_3]^{4+}$ was fully oxidized with 2 equiv NOBF_4 to $[\text{Fe}_2(\text{420})_3]^{6+}$ in an inert atmosphere box. Afterward, the solution was purged with N_2 prior to the titration to rid it of dissolved NO. Subsequently, the $[\text{Fe}_2(\text{420})_3]^{6+}$ was titrated to $[\text{Fe}_2(\text{420})_3]^{4+}$ by addition of reductant aliquots, with care taken to keep contact with ambient atmosphere to a minimum.

$[\text{Fe}(\text{TMP})_3]^{2+}$ was chosen as the reductant after considering a number of other compounds. First, it is quite soluble as its PF_6^- salt in both relevant oxidation states and it has minimal spectral interferences in the near-IR. Additionally, there was no indication of any ligand exchange between $\text{Fe}(\text{TMP})_3$ and $[\text{Fe}_2(\text{420})_3]$ during the titration. It either does not occur or, if it does, it is complete and no mixed ligand species are evident in solution (from analysis of all spectra taken during the titration and thin-layer chromatography after the titration was complete). This whole redox sequence is outlined in Scheme 1.

TABLE 1: IT Band Maxima for $[\text{Fe}_2(\text{420})_3]^{5+}$ from the Variable-Temperature Titration

| T ($^\circ\text{C}$) ^b | ν_{IT} (cm^{-1}) ^a | | |
|---------------------------------------|---|------------------------------|---|
| | first intermediate spectrum ^c | middle spectrum ^d | last intermediate spectrum ^e |
| 30 (30) | 5747 \pm 5 | 5769 \pm 4 | 5579 \pm 7 |
| 16 (15) | 5855 \pm 4 | 5812 \pm 4 | 5736 \pm 6 |
| 1 (0) | 5872 \pm 4 | 5861 \pm 4 | 5752 \pm 6 |
| -14 (-15) | 5898 \pm 5 | 5909 \pm 5 | 5769 \pm 7 |
| -28 (-30) | 5852 \pm 6 | 5837 \pm 6 | 5618 \pm 7 |

^a All values determined from the correction and curve fitting routine described in the text. ^b The cell temperature measured by inserting a thermocouple into the cell after the titration was complete. Values in parentheses are the corresponding temperature of the circulating bath. ^c The spectrum taken after addition of ~ 0.5 equiv of $[\text{Fe}(\text{TMP})_3](\text{PF}_6)_2$ to the solution of $[\text{Fe}_2(\text{420})_3]^{6+}$. ^d The spectrum taken after addition of a total of ~ 1.0 equiv of $[\text{Fe}(\text{TMP})_3](\text{PF}_6)_2$ to the solution of $[\text{Fe}_2(\text{420})_3]^{6+}$. ^e The spectrum taken after addition of a total of ~ 1.5 equiv of $[\text{Fe}(\text{TMP})_3](\text{PF}_6)_2$ to the solution of $[\text{Fe}_2(\text{420})_3]^{6+}$.

Spectral Correction Procedure. A similar approach to one described previously⁴ was used to analyze the IT band of $[\text{Fe}_2(\text{420})_3]^{5+}$. In general, each intermediate spectrum in a titration had a weighted sum of the initial and the final spectra subtracted from it. In other words, the spectrum taken at the end of the titration (of pure $[\text{Fe}_2(\text{420})_3]^{4+}$) was multiplied by a coefficient, C , and the initial spectrum (pure $[\text{Fe}_2(\text{420})_3]^{6+}$) was multiplied by $1 - C$, and these two scaled spectra were subtracted from the raw spectrum. This process was repeated at each intermediate point in the titration. A pair of weak but relatively sharp peaks at $\sim 5800 \text{ cm}^{-1}$, which are unique to the $4+$ oxidation state of the molecule, were used to determine the value of C at each intermediate point in the titration (i.e., C was chosen such that the $\sim 5800 \text{ cm}^{-1}$ peaks were absent in the final difference spectrum). Reassuringly, in all cases C was consistent with the progress of the titration estimated from the amount of $[\text{Fe}(\text{TMP})_3](\text{PF}_6)_2$ reductant added and, in the variable temperature experiment, C did not change significantly at different temperatures.

Each difference spectrum was fit to two Gaussian peaks and a constant baseline offset. One of the two Gaussians corresponds to a sharp negative peak at $\sim 5260 \text{ cm}^{-1}$, which we assign to a vibrational overtone band of the complex,⁴ and the other to the IT band itself. An explanation for the baseline offset is considered briefly later in the discussion and in more detail in the Supporting Information.

Variable Temperature Titration. Spectra were taken over the range $4650\text{--}12500 \text{ cm}^{-1}$. However, in the 5 cm path length cell the absorbance at energies higher than $\sim 11400 \text{ cm}^{-1}$ was off scale for the $4+$ oxidation state of the complex. This spectral region is remote from the maximum of the IT band, so all spectra were truncated at 11000 cm^{-1} . Fitting each truncated spectrum as described above yields values for ν_{IT} which are collected in Table 1. It should be reiterated that, since λ_i is effectively zero for the intervalence absorption of $[\text{Fe}_2(\text{420})_3]^{5+}$, ν_{IT} is directly equal to λ_o . Thus, the values in Table 1 constitute a direct measure of the outer-sphere reorganization energy associated with the electron transfer process in $[\text{Fe}_2(\text{420})_3]^{5+}$. The bandwidths that result from the fitted spectra are not included in Table 1, but they are consistently wider by a factor of ~ 1.5 than predicted by theory.¹¹ This apparent broadening is attributable to spectral effects associated with the fitting and is discussed in the Supporting Information. The difference spectrum at $30 \text{ }^\circ\text{C}$ for the midpoint in the titration along with its fit (which is typical of other spectra and their fits) are shown in Figure 1.

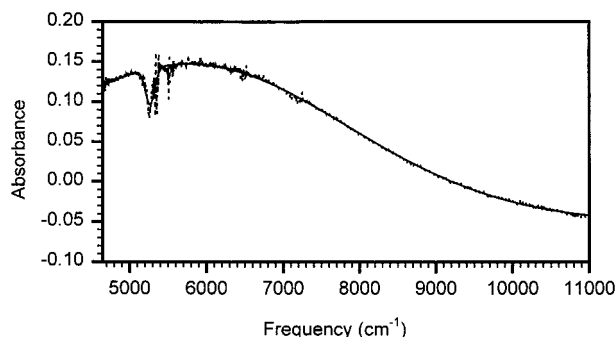


Figure 1. Near-IR spectrum of $[\text{Fe}_2(420)_3]^{5+}$. This corrected spectrum was obtained at 30 °C in acetonitrile- d_3 in a 5 cm path length cell near the middle of the variable-temperature titration described in the text. The dotted line is the corrected spectrum and the solid line is the best fit of two Gaussian peaks with a vertical baseline offset to that spectrum.

Ideally all of the data in Table 1 should be self-consistent, by which we mean that for each temperature ν_{IT} should be the same at each point in the titration. Moreover, it is expected that whatever temperature dependence there is for ν_{IT} should be smooth and monotonic. Deviations from this kind of self-consistency are flags that suggest spectral anomalies. The last three columns in Table 1 contain values of ν_{IT} found from three points in the titration, each of which corresponds to a different solution composition. The solution corresponding to the first column of data in the table contains approximately equal concentrations of $[\text{Fe}_2(420)_3]^{6+}$ and $[\text{Fe}_2(420)_3]^{5+}$, while for the second data column the solution predominantly contains $[\text{Fe}_2(420)_3]^{5+}$ (with roughly equal small, but significant amounts of $[\text{Fe}_2(420)_3]^{4+}$ and $[\text{Fe}_2(420)_3]^{6+}$ from disproportionation), and for the last column the solution contains roughly equal concentrations of $[\text{Fe}_2(420)_3]^{5+}$ and $[\text{Fe}_2(420)_3]^{4+}$. Consistent with the lower concentration of $[\text{Fe}_2(420)_3]^{5+}$, there is some scatter in the values in the first column of data; otherwise, the values in the first and second columns are in good agreement at every temperature except the lowest, *vide infra*. The last column is significantly out of line with the other two at every temperature. The data for columns 1 and 2 both exhibit the same smooth, linear increase in ν_{IT} with decreasing temperature down to the lowest temperature where, in both cases, the apparent value of ν_{IT} abruptly decreases. Through a careful analysis of the individual raw spectra, we have established to our satisfaction that the behavior of the data in the last column (i.e., the solution containing $[\text{Fe}_2(420)_3]^{4+}$ and $[\text{Fe}_2(420)_3]^{5+}$) and the last row (i.e., data at the lowest temperature) in Table 1 is attributable to spectral artifacts associated primarily with $[\text{Fe}_2(420)_3]^{4+}$. Briefly, there is a spectral interaction associated with the 2+ chromophore which is different in $[\text{Fe}_2(420)_3]^{4+}$ than in $[\text{Fe}_2(420)_3]^{5+}$. In other words, the spectrum of the 2+ chromophore is slightly different depending on whether its neighbor is 2+ or 3+. Moreover, the interaction is temperature dependent in a nonlinear way, increasing abruptly between -15 and -30 °C. One consequence is that there is a baseline offset in the difference spectra that must be taken into account in all of the fits. A full discussion of the spectral details is included in the Supporting Information, but, in the final analysis, there is adequate justification to discount the data in the last row and last column of Table 1 and to consider only the data in the first two columns at temperatures of ≥ -15 °C.

Room-Temperature Titration. In a 1 cm path length cell, the spectral window of acetonitrile- d_3 extends out to 2900 nm (3450 cm^{-1}), with only two relatively narrow regions (4517 – 4450 and 3680 – 3510 cm^{-1}) where the absorbance is off scale. Spectra at 30 °C were obtained in the 1 cm cell for comparison

TABLE 2: IT Band Maxima for $[\text{Fe}_2(420)_3]^{5+}$ from the Room-Temperature Titration

| titration progress ^b | $\nu_{\text{IT}} (\text{cm}^{-1})^a$ | |
|---------------------------------|--------------------------------------|-----------------------------|
| | truncated spectrum ^c | whole spectrum ^d |
| 1/6 | 5800 ± 20 | — ^e |
| 1/3 | 5783 ± 7 | 5830 ± 30 |
| 1/2 | 5787 ± 5 | 5870 ± 20 |
| 2/3 | 5784 ± 4 | 5810 ± 20 |
| 5/6 | 5703 ± 6 | 5800 ± 40 |
| avg | 5788 ± 6^f | 5830 ± 30 |

^a All values determined from the correction and curve fitting routine described in the text. ^b Going from $[\text{Fe}_2(420)_3]^{6+}$ to $[\text{Fe}_2(420)_3]^{4+}$. ^c Fitting the corrected spectrum in only the region from 4650 to 11000 cm^{-1} . ^d Fitting the corrected spectrum in the region 3450 – 11400 cm^{-1} minus the regions 4517 – 4450 cm^{-1} and 3680 – 3510 cm^{-1} . ^e The signal-to-noise of this spectrum was too small for it to be fit successfully. ^f Neglecting the point 5/6 of the way through the titration.

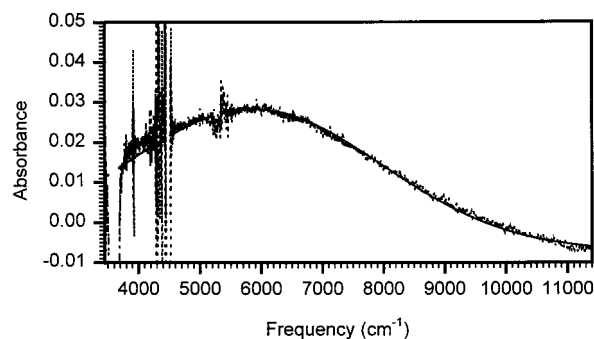


Figure 2. Broader window near-IR spectrum of $[\text{Fe}_2(420)_3]^{5+}$. This corrected spectrum differs from that shown in Figure 1 in that it was obtained in a 1 cm path length cell during the room-temperature titration carried out in acetonitrile- d_3 as described in the text. Two regions of the spectrum (4517 – 4450 cm^{-1} and 3680 – 3510 cm^{-1}) have been omitted because of off scale solvent absorptions in those regions. The dotted line is the corrected spectrum and the solid line is the best fit of two Gaussian peaks and a vertical baseline offset to that spectrum.

with the data from the thermostated cell. The correction and fitting procedures were the same except that two different energy ranges were analyzed: 11000 – 4650 cm^{-1} (the same as for the 5 cm cell) and 11400 – 3450 cm^{-1} , omitting the data from regions that were off scale. The results of the fits are given in Table 2. Concentrating on the first column of ν_{IT} values, it is evident there is excellent agreement between these data and that given in Table 1. Furthermore, the shift to lower energies late in the titration occurs in both data sets. The second column of data in Table 2 shows more scatter than the first, and the shift to lower energies late in the titration is not evident, but in general the numbers are in reasonable agreement. Figure 2 shows the corrected spectrum obtained at the midpoint in the room-temperature titration along with its fit. The fact that the shift to lower energies late in the titration is absent might result from the more symmetric nature of the data, i.e., the maximum of the band is closer to the center of the wavelength range of the data used for the fit.

Models of the Outer-Sphere Reorganizational Energy and the Temperature Dependence of λ_0 . Dielectric continuum theory¹² is frequently used to predict the absolute value of the solvent's contribution to the reorganization energy in electron transfer processes.^{1,9} In its simplest manifestation, where the donor and acceptor are treated as hard spheres, λ_0 is given by

$$\lambda_0 = (\Delta e)^2 \left(\frac{1}{D_{\text{op}}} - \frac{1}{D_s} \right) \left(\frac{1}{2a_1} + \frac{1}{2a_2} - \frac{1}{r} \right) \quad (5)$$

where Δe is the charge transferred from donor to acceptor, D_{op}

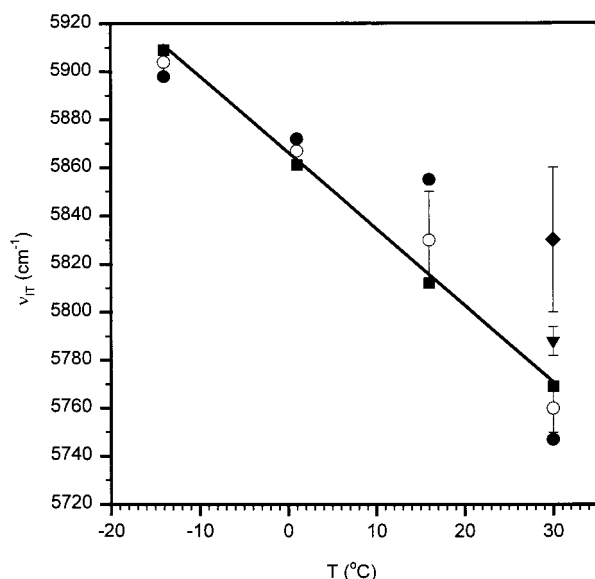


Figure 3. Temperature dependence of λ_0 . The filled circles and squares were obtained from the first and middle titration points in the variable temperature data (the first and second columns of data in Table 1), respectively. The triangle and diamond were obtained from the analysis of the truncated (4650–11000 cm^{-1}) and full (3450–11000 cm^{-1}) room-temperature data (the averages at the bottom of the first and second data columns of Table 2), respectively. The open circles are the average of the filled circles and squares and the line is a best-fit straight line to the open circles.

and D_s are the high- and low-frequency dielectric constants of the solvent, respectively, a_1 and a_2 are the radii of the donor and acceptor spheres, and r is the center-to-center separation of the donor and acceptor. Even in this highly oversimplified form, dielectric continuum theory does a surprisingly good job of predicting absolute values of λ_0 (especially for polar solvents).^{1,9} The temperature dependence of λ_0 , however, is another matter.^{3,4}

From eq 5 any temperature dependence in λ would arise from the temperature dependence of D_{op} and D_s . For polar solvents λ_0 is dominated by D_{op} (since $D_s \gg D_{\text{op}}$), and since D_{op} increases with the solvent density, it follows that λ_0 should increase with increasing T , i.e., $(\partial\lambda/\partial T)_P > 0$.

Recently Matyushov has developed and described a noncontinuum theory from which the reorganization energy for polar solvents can be calculated.¹³ This theory treats the solvent as consisting of dipolar hard spheres and, because of the discrete nature of the solvent molecules, this theory can account for molecular-based processes (such as changes in local solvent density) which are absent from continuum theory.

Figure 3 is a plot of λ_0 vs T from the data given in the second and third columns of Table 1 at $T \geq -15$ °C. The solid line is the linear least-squares fit to the average of the two data points at each temperature. The slope obtained from the fit is $-3.2 \pm 0.4 \text{ cm}^{-1}\text{K}^{-1}$. Values from the truncated and full spectra in Table 2 are also included in Figure 3 (triangles and diamonds, respectively) for comparison. We note here that, to be rigorously correct, λ_0 should be extracted from the maximum of the reduced absorption spectrum (i.e., $\epsilon \nu$ vs ν) not the “raw” spectrum (ϵ vs ν).¹⁴ In most instances, however, it makes little difference which approach is used and we, as well as others, have ignored this distinction in the past (for reasons explained in ref 4). In the current analysis, using the reduced absorption spectra instead of the “raw” spectra has a small effect on the absolute values of λ_0 extracted, but no significant effect on the slope of the line in Figure 3.

For the mixed-valence complexes such as $[\text{Fe}_2(420)_3]^{5+}$ the rate of thermal electron transfer and the nature of the IT band are determined by a number of the same parameters: λ and H_{12} , for example. In an earlier study we attempted to compare independently determined values of these parameters as obtained from spectral and electron transfer rate data gathered from a complex very similar in structure to $[\text{Fe}_2(420)_3]^{5+}$. We noted in that study that the agreement between H_{12} values determined from the two sets of data was highly dependent upon how the temperature dependence of λ was handled. Using a value of $(\partial\lambda/\partial T)_P$ calculated from continuum theory¹² made the agreement worse than assuming no temperature dependence of λ at all. In contrast, using a value of $(\partial\lambda/\partial T)_P$ calculated from the molecular-based model developed by Matyushov¹³ brought the two experimental values of H_{12} in close agreement. Unfortunately, at the time of this earlier study, no appropriate experimentally determined value of $(\partial\lambda/\partial T)_P$ was available for comparison. This absence of data largely provided the impetus for the present study.

The temperature dependence of the outer-sphere reorganization energy can be straightforwardly calculated from the Marcus continuum model, i.e., eq 5. Values of a_1 and a_2 were assumed to be equal and were calculated using eq 5 and the spectral reorganizational energy measured at room temperature, yielding $a_1 = a_2 = 4.8$ Å. Then, using temperature-dependent values of D_{op} and D_s ¹⁵ over the temperature range of interest, $(\partial\lambda/\partial T)_P$ was calculated to be $2.3 \text{ cm}^{-1}\text{K}^{-1}$. While the magnitude of this value is similar to that obtained from the data in Table 1, the two results have opposite signs. Using the spherical radii calculated for the donor and acceptor from eq 5 above (4.8 Å), application of the Matyushov model results in a value of $(\partial\lambda/\partial T)_P = -7.1 \text{ cm}^{-1}\text{K}^{-1}$. (The details of the calculation are included in the Supporting Information.) Here the sign of the temperature dependence agrees with experimental results but the magnitude is too large by a factor of ~ 2 .

Unquestionably, the physical model for the complex employed in both calculations is highly structurally unrealistic. First, the center-to-center separation of the two irons is considerably less than twice the apparent radii employed in the calculations. Moreover, this radius, 4.8 Å, is itself much less than the van der Waals radius of the donor and acceptor halves of the complex obtained crystallographically.⁶ Simply put, a model consisting of two interpenetrating hard spheres of radius 4.8 Å with a center-to-center separation of 7.6 Å is a rather unreasonable representation of $[\text{Fe}_2(420)_3]^{5+}$. That caveat notwithstanding, in the case of the dielectric continuum model calculation, improving the structural reality of the dielectric cavity changes the magnitude of $(\partial\lambda/\partial T)_P$ but not its sign. With the molecular model of Matyushov, the effects on $(\partial\lambda/\partial T)_P$ of changes in the structural model are less transparent. If, however, the same basic structural model is maintained and only the donor and acceptor radii are increased toward a more structurally realistic value, the magnitude of $(\partial\lambda/\partial T)_P$ decreases, but the sign remains negative. While the overall effect of this modification is to bring the calculated and experimental values into closer agreement, the physical model remains unreasonable. Given this fact it is probably wise to consider all of these results from theoretical calculation to be, at best, of semiquantitative value.

Conclusion

We have developed a class of compounds that is nearly ideal for studying various aspects of electron transfer reactions at the classical level. In the present paper, we use a member of this class, $[\text{Fe}_2(420)_3]^{5+}$, to analyze how the reorganizational energy

(specifically the outer-sphere component) is dependent on temperature. Assuming linearity over the temperature range studied, the derivative of the reorganization energy with temperature was found to be $-3.2 \pm 0.4 \text{ cm}^{-1}\text{K}^{-1}$. This result has the opposite sign to that predicted by continuum theory. However, a model developed by Matyushov that takes into account molecular phenomena (such as changes in local solvent density) gives semiquantitative agreement with experiment.

Acknowledgment. The authors thank Dr. Dmitry Matyushov for help in calculating the theoretical temperature dependence of λ_0 . This work was supported by the Division of Chemical Sciences, Office of Basic Energy Science, U.S. Department of Energy, under Grant DE-FG03-97ER14808.

References and Notes

- (1) (a) Newton, M. D.; Sutin, N. *Annu. Rev. Phys. Chem.* **1984**, *35*, 437. (b) Marcus, R. A.; Sutin, N. *Biochim. Biophys. Acta* **1985**, *811*, 265. (c) Wasielewski, M. R. *Chem. Rev.* **1992**, *92*, 435.
- (2) Finckh, P.; Heitele, H.; Volk, M.; Michel-Beyerle, M. E. *J. Phys. Chem.* **1988**, *92*, 6584.
- (3) (a) Liang, N.; Miller, J. R.; Closs, G. L.; *J. Am. Chem. Soc.* **1989**, *111*, 8740. (b) Dong, Y.; Hupp, J. T. *Inorg. Chem.* **1992**, *31*, 3322. (c) Krishna, K.; Kurnikov, I. V.; Beratan, D. N.; Waldeck, D. H.; Zimmt, M. B. *J. Phys. Chem. A* **1998**, *102*, 5529. (d) Vath, P.; Zimmt, M. B.; Matyushov, D. V.; Voth, G. A., submitted to *J. Phys. Chem.*
- (4) Elliott, C. M.; Derr, D. L.; Matyushov, D. V.; Newton, M. D. *J. Am. Chem. Soc.* **1998**, *120*, 11714.
- (5) Levich, V. G. *Adv. Electrochem. Electrochem. Eng.* **1966**, *4*, 249.
- (6) Serr, B. R.; Andersen, K. A.; Elliott, C. M.; Anderson, O. P. *Inorg. Chem.* **1988**, *27*, 4499.
- (7) Cruetz, C.; Taube, H. *J. Am. Chem. Soc.* **1969**, *91*, 3988.
- (8) Elliott, C. M.; Derr, D. L.; Ferrere, S.; Newton, M. D.; Liu, Y.-P. *J. Am. Chem. Soc.* **1996**, *118*, 5221.
- (9) (a) Sutin, N. *Prog. Inorg. Chem.* **1983**, *30*, 441. (b) Barbara, P. F.; Meyer, T. J.; Ratner, M. A. *J. Phys. Chem.* **1996**, *100*, 13148.
- (10) Ward, M. D. *Chem. Soc. Rev.* **1995**, *24*, 121.
- (11) Hush, N. S. *Prog. Inorg. Chem.* **1967**, *8*, 391.
- (12) Marcus, R. A. *J. Chem. Phys.* **1965**, *43*, 679.
- (13) (a) Matyushov, D. V. *Mol. Phys.* **1993**, *79*, 795. (b) Matyushov, D. V. *Chem. Phys.* **1993**, *174*, 199. (c) Matyushov, D. V.; Schmid, R. *J. Phys. Chem.* **1994**, *98*, 5152. (d) Matyushov, D. V.; Schmid, R. *Chem. Phys. Lett.* **1994**, *220*, 359.
- (14) Gould, I. R.; Noukakis, D.; Gomez-Jahn, L.; Young, R. H.; Goodman, J. L.; Farid, S. *Chem. Phys.* **1993**, *176*, 439.
- (15) (a) Moreau, C.; Douhéret, G. *J. Chem. Thermodyn.* **1976**, *8*, 403. (b) Würflinger, A. *Ber. Bunsen-Ges. Phys. Chem.* **1980**, *84*, 653.